*JETP Letters, Vol. 80, No. 3, 2004, pp. 204–207. Translated from Pis'ma v Zhurnal Éksperimental'noĭ i Teoreticheskoĭ Fiziki, Vol. 80, No. 3, 2004, pp. 231–235.*


# On the Possible Coexistence of Spiral and Collinear Structures in Antiferromagnetic $KFe(MoO_4)_2$

**L. E. Svistov[1, 3], A. I. Smirnov[1], L. A. Prozorova[1], O. A. Petrenko[2], A. Ya. Shapiro[3], and L. N. Dem'yanets[3]**

[1] *Kapitza Institute of Physical Problems, Russian Academy of Sciences, Moscow, 119334 Russia*
[2] *Department of Physics, University of Warwick, Coventry, CV4 7AL, United Kingdom*
[3] *Shubnikov Institute of Crystallography, Russian Academy of Sciences, Moscow, 117924 Russia*
Received July 7, 2004

The static and resonance properties of a quasi-two-dimensional antiferromagnet phase on a distorted triangular lattice of $KFe(MoO_4)_2$ have been experimentally studied. Magnetization curves exhibit features corresponding to the spin-flop transition in a collinear biaxial antiferromagnet and simultaneously show a magnetization plateau characteristic of a triangular spin structure. The magnetic resonance spectra also display absorption lines corresponding to the spin structures of both types. The experimental data are described in terms of a model comprising alternating weakly bound magnetic layers, in which the main two exchange integrals have different values. Below the Néel temperature ($T_N$ = 2.5 K), some of these layers possess a collinear antiferromagnetic structure, while the other layers have a triangular or spiral structure. © *2004 MAIK "Nauka/Interperiodica".*

PACS numbers: 75.50.Ee; 75.30.-m

Two-dimensional (2D) antiferromagnets on a regular triangular lattice exhibit unusual magnetic properties due to a partially frustrated antiferromagnetic exchange and the degeneracy (not vanishing in the applied magnetic field) of various spin configurations (see, e.g., [1]). The ground state corresponds to a three-sublattice magnetic structure with the spins mutually oriented at ±120° in a zero field. An important role in the magnetic structure formation is played by fluctuations, which account for the characteristic magnetization plateau (on a level of 1/3 of the saturation magnetization) in a rather broad interval of magnetic fields in the vicinity of $(1/3)H_{sat}$, where $H_{sat}$ is the saturation field. In iron molybdates of the $AFe(MoO_4)_2$ type (A = K, Na, Rb, …), magnetic $Fe^{3+}$ ($S$ = 5/2) ions are arranged on plane triangular lattices with weak exchange interaction between neighboring planes, which accounts for the quasi-2D magnetism [2, 3]. In $RbFe(MoO_4)_2$ crystals with a third-order axis (symmetry group $D_{3d}^3$), each magnetic layer has a regular triangular lattice. These crystals exhibit the properties of quasi-2D antiferromagnets on a regular triangular lattice with a ratio of the lateral and interlayer exchange integrals of 20 [3].

A different situation is observed in $KFe(MoO_4)_2$ crystals, where magnetic ordering takes place on a distorted triangular lattice. At a temperature of $T_1$ = 311 K, this compound exhibits a structural transition from a phase with the aforementioned symmetry group $D_{3d}^3$ to a monoclinic phase of $C_{2h}^3$ symmetry [4]. The size of the primitive cell along the **Z** axis perpendicular to the magnetic layers doubles, and iron ions, $Fe_I^{3+}$ and $Fe_{II}^{3+}$, appear in nonequivalent positions of two types. The **X** axis remains the second-order axis, and the **YZ** plane is still the symmetry plane (Fig. 1). Owing to this decrease in the symmetry, we may expect that, at $T < T_1$, the exchange integral $J_1$ for the neighboring iron ions arranged along the **X** axis will differ from the exchange integral $J_2$ of the neighbors arranged along other directions in the triangular structure. Thus, the triangular

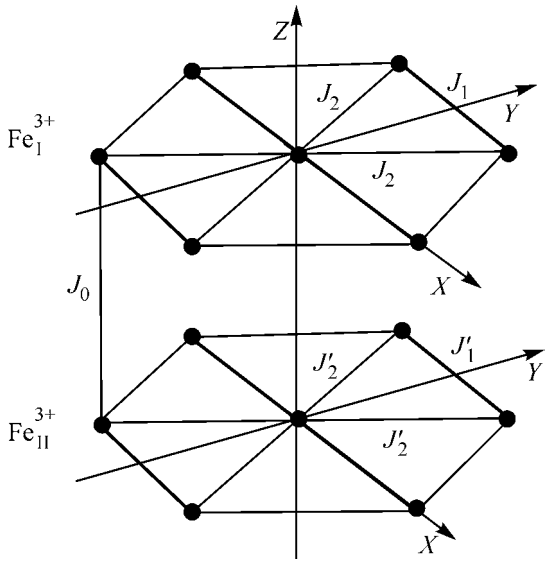


**Fig. 1.** Schematic diagram showing the arrangement of $Fe^{3+}$ magnetic ions in the crystal structure of $KFe(MoO_4)_2$.

structure of $KFe(MoO_4)_2$ crystals is distorted and the crystals contain layers of magnetic ions occurring in the nonequivalent positions of two types. According to the theoretical analysis [5], a distortion ($J_1 \neq J_2$) corresponding to $J_1 > J_2/2 > 0$ leads to the appearance of an incommensurate spiral structure with the wavevector oriented in the direction (**X** axis) of distinct exchange interaction. In contrast, for $J_2/2 > J_1 > 0$, a collinear antiferromagnetic structure becomes energetically favorable.

This study was aimed at elucidating the effect of lattice distortions on the properties of 2D antiferromagnets on a triangular lattice. For this purpose, we have studied the static and resonance magnetic properties of $KFe(MoO_4)_2$ crystals.

The experiments were performed on $KFe(MoO_4)_2$ single crystals grown by spontaneous crystallization as described in [2]. The crystals had the shape of 0.1- to 0.3-mm-thick plates with a lateral size of up to 3 mm. The face surface of the crystals coincided with the planes of iron ions. At temperatures below $T_1$, the crystal separates into three domains corresponding to the three crystallographically equivalent directions of the **X** axis in the high-temperature phase. These domains can be visually observed in polarized light. The magnetic measurements were performed with a vibrating-sample magnetometer (Oxford Instruments) and a SQUID magnetometer (Quantum Design). The magnetic resonance spectra were obtained using a set of microwave spectrometers with transmission type resonators covering the 9–150 GHz frequency range.

Figure 2 shows the temperature dependence of the magnetic susceptibility $\chi = M/H$ of $KFe(MoO_4)_2$ crystals for two orientations of the magnetic field: $\mathbf{H} \perp \mathbf{Z}$ and $\mathbf{H} \parallel \mathbf{Z}$. At a temperature of $T_N = 2.5$ K, the curves exhibit a feature corresponding to the transition to an ordered state. In the interval of temperatures 15 K $\ll T <$ 300 K, $\chi(T)$ follows the Curie–Weiss law with the characteristic constant $\Theta_{CW} = 21 \pm 2$ K. Approximation of the magnetic susceptibility by the Curie–Weiss law in the low-temperature range is shown by the dashed curve in Fig. 1. Using the Weiss constant, it is possible to estimate the average value of the exchange integral for the neighboring ions in the **XY** plane as $J = 3\Theta_{CW}/2zS(S+1) \simeq 0.6$ K ($S = 5/2$ and the number of nearest neighbors is $z = 6$). The $\Theta_{CW}$ is virtually the same for $KFe(MoO_4)_2$ and $RbFe(MoO_4)_2$ [3].

The inset in Fig. 2 shows the temperature dependences of $M/H$ for various values of the static field **H** oriented in the crystal plane ($\mathbf{H} \perp \mathbf{Z}$). The absolute values of $M/H$ for the fields 0.1 and 1 kOe are probably determined with an error of 10–50% because of a residual magnetic field of the superconducting solenoid. Open triangles indicate the aforementioned feature in the form of a magnetic susceptibility peak. The peak is observed in the region of weak fields ($0 < H < 20$ kOe) and exhibits smearing in higher fields. Above 30 kOe,

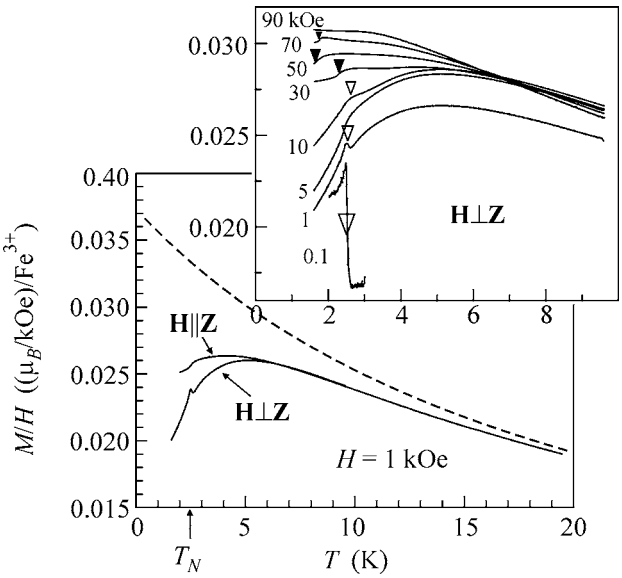


**Fig. 2.** The temperature dependence of the magnetic susceptibility $\chi = M/H$ of $KFe(MoO_4)_2$ crystals (for the sake of clarity, the curves for **H** = 0.1 and 1 kOe in the inset are shifted along the ordinate axis).

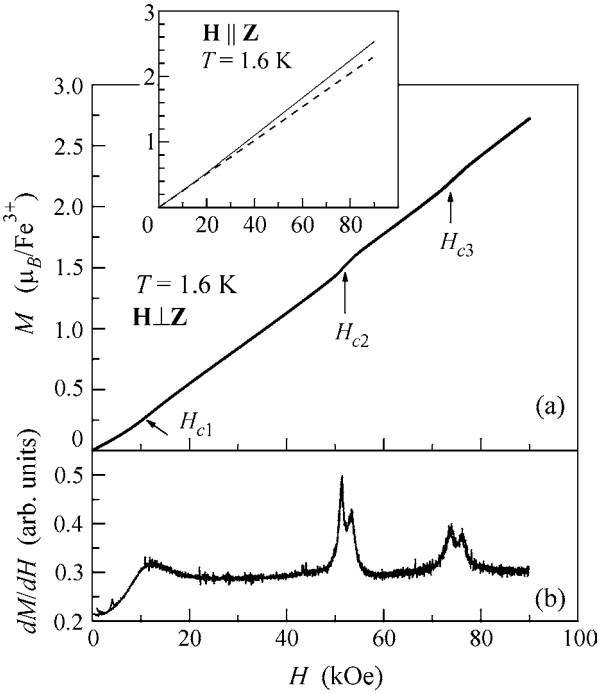


**Fig. 3.** (a) The magnetization curve $M(H)$ and (b) its derivative measured for a $KFe(MoO_4)_2$ crystal for $\mathbf{H} \perp \mathbf{Z}$. The inset shows the $M(H)$ curve observed for $\mathbf{H} \parallel \mathbf{Z}$ (the dashed line is tangent to the $M(H)$ curve in the region of small fields). All measurements were performed at $T = 1.6$ K.

the $M(T)$ curves exhibit variations in the form of steps, which are indicated by black triangles in the inset in Fig. 2. In addition, it should be noted that these curves exhibit a flattened maximum characteristic of low-dimensional antiferromagnets [6].

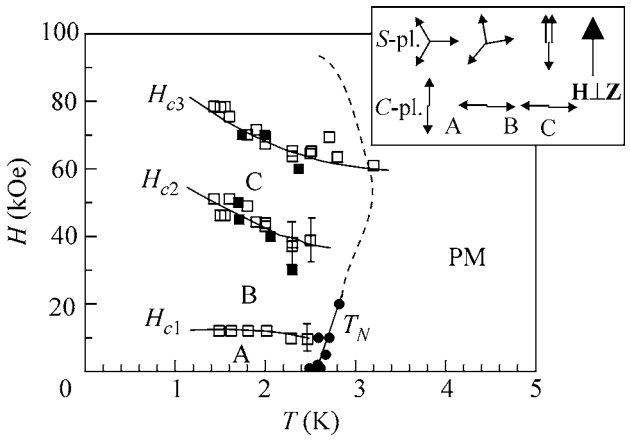


**Fig. 4.** The $H$ versus $T$ diagrams of the magnetic states observed for $\mathbf{H} \perp \mathbf{Z}$, showing the boundaries of the region of magnetic phases determined from (□) the $M(H)$ and (■) the $M(T)$ measurements. Black circles indicate the values of the Néel temperature. The inset shows the probable spin structures of the magnetic phases A, B, and C.

Figure 3a shows the $M(H)$ curves measured at $T$ = 1.6 K for two orientations of the applied magnetic field. For $\mathbf{H} \perp \mathbf{Z}$, there are three features in these curves. Near $H = H_{c1}$ = 12.5 kOe, there is a change in the slope of the $M(H)$ curve and the corresponding peak in the derivative $dM/dH$ (Fig. 3b). The two other features are observed at $H_{c2}$ = 52 kOe and $H_{c3}$ = 76 kOe, where the derivative $dM/dH$ exhibits sharp peaks. For $\mathbf{H} \parallel \mathbf{Z}$, the only special feature is an increase in the derivative in a field of 20–30 kOe. The slope of $M(H)$ in the region of lower fields was 0.9 of that in the region of higher fields ($H$ > 50 kOe).

Figure 4 presents the $H$ versus $T$ diagram showing variation of the fields of magnetic phase transitions $H_{c1}$, $H_{c2}$, and $H_{c3}$ determined for the features in the $M(H)$ and $M(T)$ curves and in the Néel temperature $T_N$ determined by the position of the magnetic susceptibility peak.

The relation between susceptibilities, $\chi_\perp > \chi_\parallel$, observed in the fields above 20 kOe (where the difference reaches 5%) indicates that the "hard" magnetization direction is near the **Z** axis. In concluding so, we proceed from the fact that magnetic susceptibility exhibits a minimum along the hard axis in both collinear and triangular structures. The existence of a magnetic anisotropy with the hard axis oriented close to the **Z** axis is also confirmed by data on the paramagnetic resonance of $Fe^{3+}$ ions at $T > T_N$ [7]. It should be noted that the absence of a high-order axis also implies the presence of another, so-called "medium" magnetization axis perpendicular to the hard axis.

The results of the experiments presented above show that the number of features of comparable magnitude on the $M(H)$ curve exceeds their number expected for both collinear and spiral structures on a distorted triangular lattice. Indeed, only one (spin-flop) feature is expected for the collinear structure, and two such features (at the beginning and end of the magnetization plateau) are expected for the triangular and spiral structures [3, 8]. As was indicated above, the magnetic structure of $KFe(MoO_4)_2$ comprises two types of weakly bound alternating nonequivalent planes of magnetic ions. For this reason, we will consider a hypothetical model in which a collinear antiferromagnetic structure is formed in planes of the first type ($C$ planes) and a spiral spin structure, in planes of the second type ($S$ planes).

Within the framework of this model, the low-field feature at $H = H_{c1}$ can be considered as a reorientational transition in the $C$ planes, which is related to rotation of the spin structure in the plane perpendicular to the hard axis. When the field is parallel to the easy axis, such a reorientation must have the character of spin flop, leading to a jump in the $M(H)$ curve. The feature observed in experiment exhibits a smoothened shape, which is explained by the presence of three domains with different orientations of their easy axes, on the one hand, and by a slight deviation of the easy axis from the **Y** axis in the **YZ** plane, on the other hand. This feature will be referred to below as a feature of the spin-flop type.

At the same time, the presence of phase transitions in the fields $\mathbf{H}_{c2}$ and $\mathbf{H}_{c3}$ on both sides of $(1/3)H_{sat}$ is characteristic of the 120° triangular structure ($J_1 = J_2$) [1, 3, 9] and the spiral structure on a distorted triangular lattice [8]. Note that the $(1/3)H_{sat}$ value apparently falls within the interval between $\mathbf{H}_{c2}$ and $\mathbf{H}_{c3}$. Indeed, judging from the $H_{sat}$ value, this field has to be approximately on the same order of magnitude as in $RbFe(MoO_4)_2$ crystals, where saturation is reached at 186 kOe [9]. The inset in Fig. 4 shows the scheme of probable spin configurations for the field orientation $\mathbf{H} \perp \mathbf{Z}$. Our experiments did not reveal significant features during the transition from the paramagnetic to the ordered phase in the range of fields above 40 kOe. The probable position of such a transition or crossover between the above phases is depicted by the dashed line in Fig. 4.

The presence of hard-axis anisotropy suggests that a structure of the umbrella type is formed in the $S$ planes at the $\mathbf{H} \parallel \mathbf{Z}$ orientation, while the $C$ planes exhibit spin reorientation caused by a deviation of the hard axis from the **Z** axis in the **YZ** plane. The strong field dependence of the amplitude of the susceptibility peak in the region of weak fields probably corresponds to a small ferromagnetic moment, on the order of $10^{-4}\mu_B$ per $Fe^{3+}$ ion.

Figure 5 shows the spectra of magnetic resonance measured at $T$ = 1.3 K in the field **H** oriented parallel and perpendicular to the **Z** axis (i.e., significantly below $T_N$). Since the crystals studied at a temperature below 311 K exhibit the formation of domains of three types with different orientations of the $X$ axis, the antiferromagnetic resonance (AFMR) line is usually split into three peaks with relative intensities strongly depending

on the realization of the domain structure in a particular sample. When the field is oriented parallel to the **Z** axis, all domains occur in approximately equivalent conditions and the observed absorption lines are not split. For this field orientation, there are four AFMR branches, one of which has a small dispersion (Fig. 5a). Figure 5b shows the spectra of magnetic resonance for five samples measured using the field oriented in the **XY** plane, with uncontrolled mutual orientation of the **Y** and **H** axes. In this case, the AFMR spectrum also displays four branches. The $\nu_1$ branch (for which additional experiments with rotation of the sample showed the most pronounced dependence of the resonance frequency on the field orientation in the **XY** plane) is characterized by a broad distribution of resonance fields and frequencies in the $\nu$ versus $H$ plane. In a zero field, the AFMR frequencies are $\nu_1^0 = 36 \pm 5$ GHz, $\nu_{3,4}^0 = 78 \pm 3$ GHz, and $\nu_2^0 = 123 \pm 3$ GHz.

In the triangular spin structure of $RbFe(MoO_4)_2$ crystals, the $\nu_{3,4}$ frequencies are close and exhibit similar field dependences with two branches of the magnetic resonance spectrum in the triangular spin structure [3]. In the case of $KFe(MoO_4)_2$ crystals, the behavior of $\nu_1(H)$ and $\nu_2(H)$ is characteristic of a collinear antiferromagnet with two anisotropy axes [10]. In Fig. 5, dotted curves show the AFMR spectrum calculated assuming that the $\nu_{1,2}(H)$ branches are determined by the homogeneous spin oscillations in the $C$ planes [10], while $\nu_{3,4}(H)$ branches reflect oscillations in the $S$ planes [3]. The interaction between the $C$ and $S$ planes was ignored.

Using the above zero-field AFMR frequencies, it is possible to estimate the values of magnetic anisotropy constants $D$ in the microscopic theory (for the model Hamiltonian presented in [3]): $D_S \approx 0.25$ K and $D_C = 0.36$ K. The difference between $\nu_1^0$ and $\nu_2^0$ is explained by the biaxial character of anisotropy in the $KFe(MoO_4)_2$ crystals. Using these values, one can find that the magnetic anisotropy constant $D_C''$ for the medium magnetization axis in the $C$ planes is approximately ten times as small as the $D_C$ value. This anisotropy axis is parallel to the $X$ axis. The AFMR spectrum of $S$ planes was calculated disregarding the crystal anisotropy in the easy plane.

Thus, the obtained spectrum of magnetic resonance corresponds to a combination of the spectrum of a collinear biaxial antiferromagnet and the spectrum of a spiral or triangular antiferromagnet.

Summarizing the results presented above and generalizing the results of analysis, we conclude that the model of a magnetic structure comprising magnetic planes of two types—with collinear and spiral order—adequately describes the whole body of the static and resonance magnetic properties of $KFe(MoO_4)_2$ crystals. However, this statement is conjectural in nature, since the model does not take into account the interplanar interaction capable of leading to additional phase transitions and lines in the magnetic resonance spectra (see [3]). The proposed exotic model can be verified in experiments on the determination of the magnetic structure using neutron scattering.

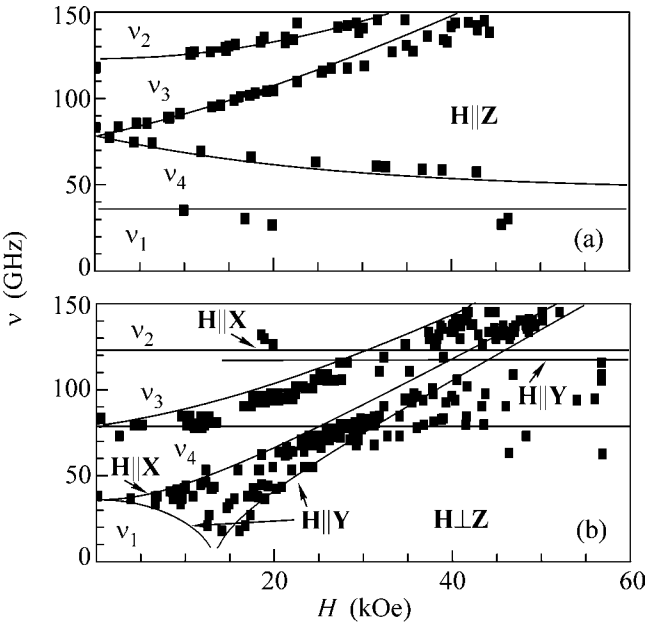


**Fig. 5.** Plots of the AFMR frequencies versus magnetic field for (a) $\mathbf{H} \perp \mathbf{Z}$ and (b) $\mathbf{H} \parallel \mathbf{Z}$ measured at $T = 1.6$ K.

We are grateful to V.I. Marchenko and S.S. Sosin for fruitful discussions. This study was supported by the Russian Foundation for Basic Research, project no. 04-02-17294.

## REFERENCES

1. S. E. Korshunov, J. Phys. C: Solid State Phys. **19**, 5927 (1986).
2. R. F. Klevtsova and P. V. Klevtsov, Kristallografiya **15**, 953 (1970) [Sov. Phys. Crystallogr. **15**, 829 (1970)].
3. L. E. Svistov, A. I. Smirnov, L. A. Prozorova, *et al.*, Phys. Rev. B **67**, 094434 (2003).
4. G. G. Kraĭnyuk, A. I. Otko, and A. E. Nosenko, Izv. Akad. Nauk SSSR, Ser. Fiz. **47**, 758 (1983).
5. W. Zhang, W. M. Saslow, and M. Gabay, Phys. Rev. B **44**, 5129 (1991).
6. L. J. de Jongh and A. R. Miedema, Adv. Phys. **50**, 947 (2001).
7. L. E. Svistov, A. I. Smirnov, L. A. Prozorova, *et al.*, Results of EPR Investigations (to be published soon).
8. T. Ono, H. Tanaka, H. Aruga Katori, *et al.*, Phys. Rev. B **67**, 104431 (2003).
9. T. Inami, Y. Ajito, and T. Goto, J. Phys. Soc. Jpn. **65**, 2374 (1996).
10. T. Nagamiya, K. Yosida, and R. Kubo, Adv. Phys. **4**, 1 (1955).

*Translated by P. Pozdeev*